

Elastic lateral-distortional buckling of I-beams and the Meck Plot

Tadeh Zirakian* and Seyed Ali Nojoumi

Department of Civil and Environmental Engineering, University of California, Los Angeles,
Los Angeles, CA 90095-1593, USA

(Received December 24, 2009, Accepted October 13, 2010)

Abstract. Meck Plot is an adapted version of the well-known Southwell method to the case of lateral-torsional buckling, which indeed reflects the physical inter-dependence of lateral flexure (lateral displacement) and torsion (rotation) in the structure. In the recent reported studies, it has been shown experimentally and theoretically that lateral displacement of an I-beam undergoing elastic lateral-distortional mode of buckling is interestingly directly coupled with other various deformation characteristics such as web transverse strain, web longitudinal strain, vertical deflection, and angles of twist of top and bottom flanges, and consequently good results have been obtained as a result of application of the Meck's method on lateral displacement together with each of the aforementioned deformation variables. In this paper, it is demonstrated that even web transverse and longitudinal strains, vertical deflection, and angles of twist of top and bottom flanges of an I-beam undergoing elastic lateral-distortional buckling are two-by-two directly coupled and the application of the Meck Plot on each pair of these deformation variables may still yield reliable predictions for the critical buckling load.

Keywords: lateral-distortional buckling; elasticity; I-beams; deformation, characteristics; Meck Plot.

1. Introduction

Meck (1977) proposed a skewed version of the standard Southwell Plot (Southwell 1932) for experimental determination of the buckling load in problems of lateral-torsional buckling. He believed that the problem of lateral-torsional buckling is more complicated than flexural buckling and it is necessary to consider both lateral displacement (δ_L) and rotation (ϕ) of the section. In fact, Meck's version of the Southwell Plot may be seen as reflecting the physical inter-dependence of lateral flexure and torsion in the structure under test, and is regarded as the "natural" generalization of the Southwell Plot to the case of lateral-torsional buckling (Mandal and Calladine 2002).

Based on his analysis of lateral-torsional buckling, Meck suggested to make a plot of (ϕ/M) against δ_L , and another of (δ_L/M) against ϕ , and that the respective slopes of the straight-line portions of these two plots will be $1/\alpha$ and $1/\beta$, and consequently M_{cr} will be the geometric mean of the slopes of the two plots (Eq. (1)).

$$M_{cr} = (\alpha\beta)^{0.5} \quad (1)$$

*Corresponding author, Ph.D. Student, E-mail: tzirakian@ucla.edu

In addition, Mandal and Calladine (2002) demonstrated that in general δ_L tends to be proportional to ϕ as deformations increase in case of lateral-torsional buckling and came up with the following equation.

$$\delta_{Lc}/\phi_c \rightarrow (\alpha/\beta)^{0.5} + const. \quad (2)$$

In a recent reported study on lateral-distortional buckling of I-beams (Zirakian 2008), as a result of analysis of the experimental data it was interestingly found that in this mode of buckling, lateral displacement (δ_L) tends to be proportional to web transverse strain (ε_T) as deformations increase. This key finding was also verified theoretically by taking advantage of the theoretical model developed for lateral-torsional buckling mode. Consequently, based on this finding, good predictions were obtained for the critical buckling load as a result of application of Meck's method on δ_L and ε_T . It should be noted that lateral-distortional buckling mode is evidently more complicated than lateral-torsional buckling mode, since in the distortional mode lateral instability of the beam is accompanied by cross-section distortion.

In continuation of the aforementioned experimental research work, a further step was taken lately (Zirakian 2010) and the relationship between lateral displacement (δ_L) and various deformation variables, viz. web transverse strain (ε_T), web longitudinal strain (ε_L), vertical deflection (δ_V), and angles of twist of top and bottom flanges (θ_{TF} and θ_{BF}), in I-beams undergoing elastic lateral-distortional mode of buckling was investigated through finite element studies. In this study (Zirakian 2010), plots of δ_L against ε_T , ε_L , δ_V , θ_{TF} , and θ_{BF} were made and it was observed that the data-points in all cases, apart from the initial few, generally lie on straight lines. In other words, δ_L was found to be proportional to ε_T , ε_L , δ_V , θ_{TF} , and θ_{BF} . Time and again, by taking advantage of Meck's (Meck 1977, Mandal and Calladine 2002) approach proposed for the case of lateral-torsional buckling mode, these proportionality findings were accompanied by theoretical verifications. Finally, the application of the Meck Plot method resulted in reliable predictions for the critical buckling load in all considered cases. As a result, it was shown that in Meck's plotting method lateral displacement (δ_L) can even be used together with other deformation variables, i.e., ε_T , ε_L , δ_V , θ_{TF} , and θ_{BF} , and still good and reliable predictions may be obtained for the critical buckling load.

In the present research work, one further step is taken in order to complement and generalize the

Table 1 Considered combinations of deformation variables

Case	First deformation variable (d.v.1)	Second deformation variable (d.v.2)
1	web transverse strain (ε_T)	web longitudinal strain (ε_L)
2	web transverse strain (ε_T)	vertical deflection (δ_V)
3	web transverse strain (ε_T)	angle of twist of top flange (θ_{TF})
4	web transverse strain (ε_T)	angle of twist of bottom flange (θ_{BF})
5	web longitudinal strain (ε_L)	vertical deflection (δ_V)
6	web longitudinal strain (ε_L)	angle of twist of top flange (θ_{TF})
7	web longitudinal strain (ε_L)	angle of twist of bottom flange (θ_{BF})
8	vertical deflection (δ_V)	angle of twist of top flange (θ_{TF})
9	vertical deflection (δ_V)	angle of twist of bottom flange (θ_{BF})
10	angle of twist of top flange (θ_{TF})	angle of twist of bottom flange (θ_{BF})

prior research results. Accordingly, the relationship between web transverse strain (ε_T), web longitudinal strain (ε_L), vertical deflection (δ_v), and angles of twist of top and bottom flanges (θ_{TF} and θ_{BF}), including ten cases as shown in Table 1, is firstly examined in case of elastic lateral-distortional buckling of I-beams with various initial geometrical imperfections, support conditions, cross-sections, and types of loading, and subsequently the use of the Meck Plot method in all of the considered cases is investigated.

2. Finite element analysis

Finite element analysis using ABAQUS (2005) was employed in this work to develop lateral-distortional buckling solutions and capture the various deformation variables of the considered I-beams. The details of the three studied structures including the support conditions, dimensions, and loading configurations are provided in Table 2.

The cross-section components of the I-beam were modeled using the S4R5 shell element. No transverse stiffeners were considered over the beam span; that is, the web was modeled as unstiffened. Moreover, the material properties adopted for the beam were $E = 200$ GPa, $\nu = 0.3$, $F_y = 345$ MPa, and $G = 0.385E$.

Geometric nonlinear and linear elastic material analysis solutions were conducted on the beams with curvature and twist as initial geometrical imperfections. The details of the applied initial lateral crookedness and twist of the beams are given in Table 3. It should be noted that the considered initial out-of-plumbness imperfection in case of the simply supported I-beam was

Table 2 Details of the considered Ibeams

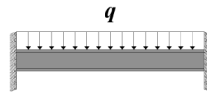
Beam	Loading and support conditions	h_w (mm)	t_w (mm)	b_{ft} (mm)	b_{fb} (mm)	t_f (mm)	L (mm)
B1		900	5	240	240	20	7000
B2		600	5	100	210	20	7500
B3		700	5	210	100	20	5000

Table 3 Applied initial imperfections of the Ibeams

Beam	Location	δ_{Lo} (mm)	δ_{vo} (mm)	ϕ_o (rad)
B1	midspan	20	20	0.04363
B2	midspan	7.5	7.5	0.04363
B3	free end	10	10	0.02618

Table 4 Ratios of M_{LDB}/M_y and M_{LDB}/M_{LTB}

Beam	M_{LDB}/M_y	M_{LDB}/M_{LTB}
B1	0.72	0.82
B2	0.88	0.90
B3	0.62	0.84

scaled to $L/350$, which is somewhat larger than the accepted fabrication tolerance of $L/1000$. In fact, the intention was to assess the deleterious effect of a larger initial crookedness than the tolerance limit would permit. This was considered to represent an extreme case of crookedness in practice.

The various considered deformation variables were measured at the midspan of the simply supported ($B1$) and fixed-ended ($B2$) as well as the free end of the cantilever ($B3$) beams.

Lastly, the considered I-beams had compact flanges and slender webs, and consequently underwent lateral-distortional mode of buckling. The M_{LDB}/M_y and M_{LDB}/M_{LTB} ratios are provided in Table 4. M_{LDB} was estimated by applying the Southwell Plot on the lateral displacement of the top flange at the measurement location. From the table, the occurrence of elastic as well as distortional buckling is evident.

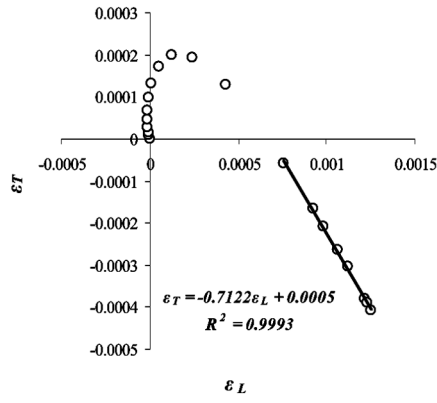
3. Relationship between deformation variables

As it was mentioned before, in the previous study (Zirakian 2010), it was demonstrated that lateral displacement (δ_L) of the I-beams undergoing elastic lateral-distortional buckling is directly coupled with web transverse strain (ε_T), web longitudinal strain (ε_L), vertical deflection (δ_V), and angles of twist of top and bottom flanges (θ_{TF} and θ_{BF}), and accordingly δ_L was used in the Meck plots together with the other aforementioned deformation variables. The first objective of this comprehensive study is to examine the relationship between each of two of ε_T , ε_L , δ_V , θ_{TF} , and θ_{BF} without considering the commonly-used deformation characteristic, i.e., δ_L .

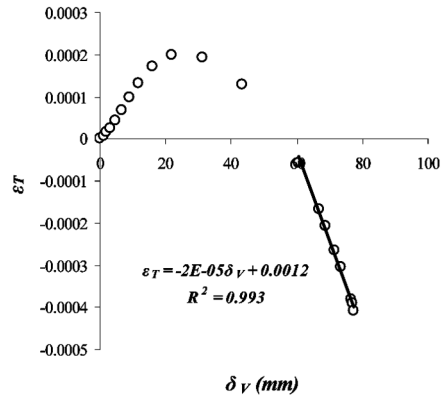
To achieve the aims of this part of the study, $d.v.1$ is straightforwardly plotted against $d.v.2$. The respective plots of the ten considered cases for $B1$ are provided in Fig. 1. Similar plots for $B2$ and $B3$ are obtained; however, the results of $B1$ are only presented for brevity. The linear equations obtained using the least squares method as well as the respective R-squared values are also displayed in the figures.

As it is seen in the figures, the data points in all cases, apart from the initial few, eventually lie on straight lines and the two deformation variables become proportional to each other. The R-Squared values also indicate that the resulting lines match pretty well with the data points.

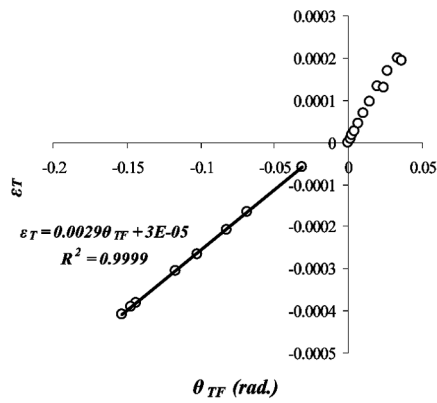
In accordance with the experimental and theoretical observations and results of the previous studies (Zirakian 2008, 2010), these proportionality findings now enable us to apply the Meck Plot method and confidently expect to obtain reliable predictions for the critical buckling moment in all cases. This is indeed the second objective and the main focus of this paper which is discussed in the next section.



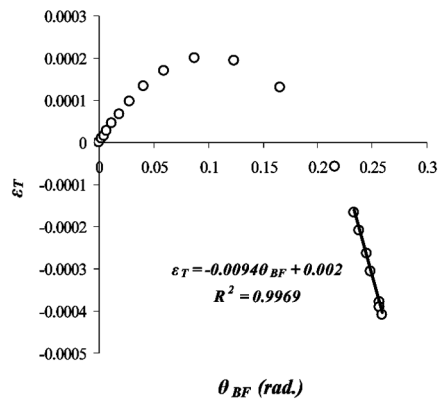
(a) ε_T vs. ε_L



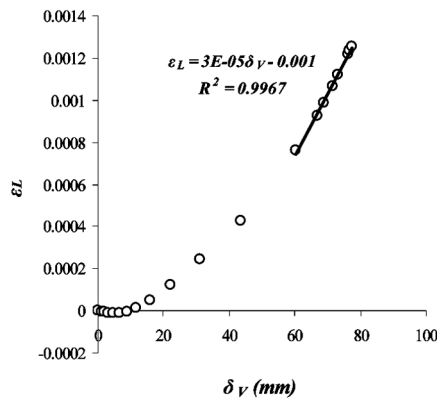
(b) ε_T vs. δ_V



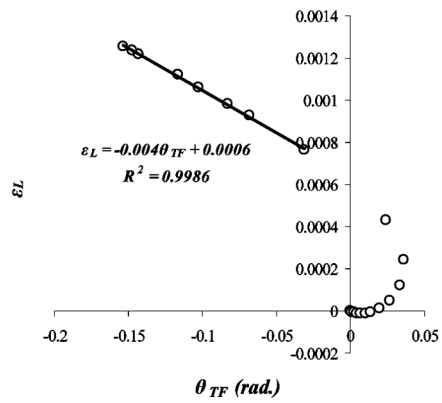
(c) ε_T vs. θ_{TF}



(d) ε_T vs. θ_{BF}



(e) ε_L vs. δ_V



(f) ε_L vs. θ_{TF}

Fig. 1 Relationship between deformation variables (B1)

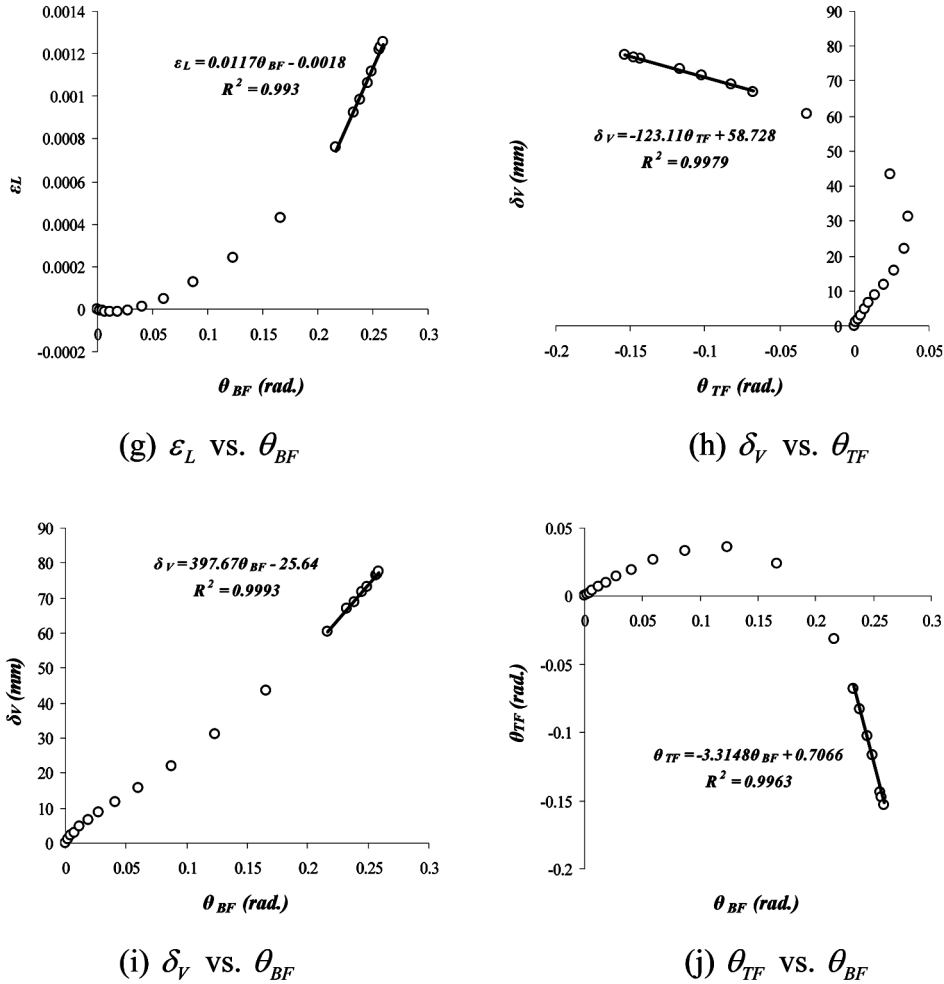


Fig. 1 Continued

4. Application of the Meck Plot method

According to Meck’s prescription, plots are made of $d.v.2/M$ versus $d.v.1$ and of $d.v.1/M$ versus $d.v.2$ for the ten considered cases for $B1$, $B2$, and $B3$. It is found that the points in all cases tend to eventually lie on a straight line, and according to Eq. (1), the product of the inverse slopes of the straight-line portions in the two aforementioned plots is equal to the square of the critical moment.

In addition, based on the linear relationship between the deformation variables in all cases as well as the results of the previous studies (Zirakian 2008, 2010), we may take advantage of the theoretical model developed for the case of lateral-torsional buckling and re-write Eq. (2) in a general form as

$$d.v.1/d.v.2 \rightarrow (\alpha/\beta)^{0.5} + const. \tag{3}$$

Table 5 Linear equations obtained from plots and Eq. (3) - B1

Case	Linear equations from plots	$d.v.1/d.v.2 \rightarrow (\alpha/\beta)^{0.5} + const.$
1	$\varepsilon_T = (7.12E - 01)\varepsilon_L + (5.00E - 04)$	$\varepsilon_T/\varepsilon_L \rightarrow (7.64E - 01) + const.$
2	$\varepsilon_T = (2.00E - 05)\delta_V + (1.20E - 03)$	$\varepsilon_T/\delta_V \rightarrow (2.30E - 05) + const.$
3	$\varepsilon_T = (2.90E - 03)\theta_{TF} + (3.00E - 05)$	$\varepsilon_T/\theta_{TF} \rightarrow (3.10E - 03) + const.$
4	$\varepsilon_T = (9.40E - 03)\theta_{BF} + (2.00E - 03)$	$\varepsilon_T/\theta_{BF} \rightarrow (1.03E - 02) + const.$
5	$\varepsilon_L = (3.00E - 05)\delta_V - (1.00E - 03)$	$\varepsilon_L/\delta_V \rightarrow (3.30E - 05) + const.$
6	$\varepsilon_L = (4.00E - 03)\theta_{TF} + (6.00E - 04)$	$\varepsilon_L/\theta_{TF} \rightarrow (4.20E - 03) + const.$
7	$\varepsilon_L = (1.17E - 02)\theta_{BF} - (1.80E - 03)$	$\varepsilon_L/\theta_{BF} \rightarrow (1.25E - 02) + const.$
8	$\delta_V = (1.23E + 02)\theta_{TF} + (5.87E + 01)$	$\delta_V/\theta_{TF} \rightarrow (1.21E + 02) + const.$
9	$\delta_V = (3.98E + 02)\theta_{BF} - (2.56E + 01)$	$\delta_V/\theta_{BF} \rightarrow (3.99E + 02) + const.$
10	$\theta_{TF} = (3.31E + 00)\theta_{BF} + (7.07E - 01)$	$\theta_{TF}/\theta_{BF} \rightarrow (3.87E + 00) + const.$

Table 6 Linear equations obtained from plots and Eq. (3) - B2

Case	Linear equations from plots	$d.v.1/d.v.2 \rightarrow (\alpha/\beta)^{0.5} + const.$
1	$\varepsilon_T = (9.14E + 00)\varepsilon_L - (4.96E - 04)$	$\varepsilon_T/\varepsilon_L \rightarrow (9.71E + 00) + const.$
2	$\varepsilon_T = (5.90E - 04)\delta_V - (7.75E - 04)$	$\varepsilon_T/\delta_V \rightarrow (6.51E - 04) + const.$
3	$\varepsilon_T = (2.84E - 02)\theta_{TF} - (2.12E - 05)$	$\varepsilon_T/\theta_{TF} \rightarrow (2.87E - 02) + const.$
4	$\varepsilon_T = (1.68E - 01)\theta_{BF} + (1.88E - 04)$	$\varepsilon_T/\theta_{BF} \rightarrow (1.63E - 01) + const.$
5	$\varepsilon_L = (6.22E - 05)\delta_V - (2.63E - 05)$	$\varepsilon_L/\delta_V \rightarrow (6.58E - 05) + const.$
6	$\varepsilon_L = (3.37E - 03)\theta_{TF} + (4.89E - 05)$	$\varepsilon_L/\theta_{TF} \rightarrow (3.17E - 03) + const.$
7	$\varepsilon_L = (2.01E - 02)\theta_{BF} + (7.33E - 05)$	$\varepsilon_L/\theta_{BF} \rightarrow (1.82E - 02) + const.$
8	$\delta_V = (5.21E + 01)\theta_{TF} - (1.23E + 00)$	$\delta_V/\theta_{TF} \rightarrow (4.70E + 01) + const.$
9	$\delta_V = (3.13E + 02)\theta_{BF} - (1.61E + 00)$	$\delta_V/\theta_{BF} \rightarrow (2.71E + 02) + const.$
10	$\theta_{TF} = (5.81E + 00)\theta_{BF} + (7.37E - 03)$	$\theta_{TF}/\theta_{BF} \rightarrow (5.53E + 00) + const.$

Table 7 Linear equations obtained from plots and Eq. (3) - B3

Case	Linear equations from plots	$d.v.1/d.v.2 \rightarrow (\alpha/\beta)^{0.5} + const.$
1	$\varepsilon_T = (8.86E + 00)\varepsilon_L + (9.84E - 02)$	$\varepsilon_T/\varepsilon_L \rightarrow (8.61E + 00) + const.$
2	$\varepsilon_T = (1.78E - 01)\delta_V - (3.09E + 00)$	$\varepsilon_T/\delta_V \rightarrow (2.77E - 01) + const.$
3	$\varepsilon_T = (1.40E + 01)\theta_{TF} - (2.78E - 02)$	$\varepsilon_T/\theta_{TF} \rightarrow (1.40E + 01) + const.$
4	$\varepsilon_T = (1.41E + 01)\theta_{BF} - (8.24E - 02)$	$\varepsilon_T/\theta_{BF} \rightarrow (1.43E + 01) + const.$
5	$\varepsilon_L = (2.11E - 02)\delta_V - (3.80E - 01)$	$\varepsilon_L/\delta_V \rightarrow (3.32E - 02) + const.$
6	$\varepsilon_L = (1.62E + 00)\theta_{TF} - (1.53E - 02)$	$\varepsilon_L/\theta_{TF} \rightarrow (1.69E + 00) + const.$
7	$\varepsilon_L = (1.54E + 00)\theta_{BF} - (1.90E - 02)$	$\varepsilon_L/\theta_{BF} \rightarrow (1.63E + 00) + const.$
8	$\delta_V = (7.53E + 01)\theta_{TF} + (1.74E + 01)$	$\delta_V/\theta_{TF} \rightarrow (4.84E + 01) + const.$
9	$\delta_V = (7.61E + 01)\theta_{BF} + (1.71E + 01)$	$\delta_V/\theta_{BF} \rightarrow (4.91E + 01) + const.$
10	$\theta_{TF} = (9.45E - 01)\theta_{BF} - (2.06E - 03)$	$\theta_{TF}/\theta_{BF} \rightarrow (9.69E - 01) + const.$

Table 8 Meck Plot predictions

Case	B1	B2	B3
	M_{Meck}/M_u	q_{Meck}/q_u	P_{Meck}/P_u
1	1.02	1.14	1.04
2	1.07	1.19	1.67
3	0.95	1.05	1.07
4	1.07	1.03	1.08
5	1.03	1.29	1.65
6	0.97	1.15	1.05
7	1.17	1.11	1.04
8	1.10	1.20	1.67
9	1.17	1.16	1.68
10	1.20	1.04	1.09

where α and β are the reciprocal slopes of the straight-line portions of plots of $d.v.2/M$ versus $d.v.1$ and of $d.v.1/M$ versus $d.v.2$, respectively. The two sets of linear equations for $B1$, $B2$, and $B3$ obtained from the two approaches, are summarized in Tables 5, 6, and 7, respectively.

From the tables it is evident that, regardless of a few cases in Table 7 where δ_V is used with the other deformation variables, in almost all cases the linear equations obtained from the plots are approximated well by Eq. (3). In other words, the agreement between the estimates of $(\alpha/\beta)^{0.5}$ in Eq. (3) and the equivalent values in the obtained linear equations from the plots, which are underlined in the tables as well, is generally good. This agreement, in fact, indicates that: first, Eq. (3) which is the general and adapted form of Eq. (2) to the case of lateral-distortional buckling works well by yielding good results; and second, the agreement serves as a theoretical verification for the validity of our findings regarding the proportionality between the deformation variables.

Finally, the ratios between Meck Plot predictions as well as the ultimate failure loads are given in Table 8 for the ten considered cases for $B1$, $B2$, and $B3$. In spite of some scatter in the results due to application of various deformation variables, it can be seen from the table that the “modified” Meck Plot method has yielded reliable predictions for elastic lateral-distortional buckling of the I-beams. However, it is notable that in case of the cantilever beam ($B3$), the Meck Plot predictions are relatively large compared to the ultimate failure loads in cases where δ_V is used with the other deformation variables.

5. Discussion

It is important to note that the proportionality between the various deformation variables is the key finding of the present research which finally results in a great extension in the application of the extrapolation techniques.

The possibility of extension of theoretical model developed for lateral-torsional buckling mode to the case of lateral-distortional buckling may be considered as another feature of this study, since it provides a theoretical verification of the key findings of the present research.

Table 9 Comparison of Meck Plot with Southwell, Massey, and Modified Plot predictions

Beam	Ratio of plotting methods	Case									
		1	2	3	4	5	6	7	8	9	10
B1	$\frac{\text{Southwell}}{\text{Meck}}$	1.10	1.05	1.18	1.05	1.09	1.15	0.96	1.02	0.96	0.93
	$\frac{\text{Massey}}{\text{Meck}}$	1.02	0.97	1.09	0.97	1.01	1.07	0.89	0.95	0.89	0.86
	$\frac{\text{Modified}}{\text{Meck}}$	1.02	0.97	1.09	0.97	1.00	1.06	0.89	0.94	0.89	0.86
B2	$\frac{\text{Southwell}}{\text{Meck}}$	0.89	0.86	0.98	0.99	0.79	0.89	0.92	0.85	0.88	0.98
	$\frac{\text{Massey}}{\text{Meck}}$	0.92	0.88	1.00	1.02	0.81	0.91	0.94	0.87	0.90	1.01
	$\frac{\text{Modified}}{\text{Meck}}$	0.92	0.88	1.00	1.02	0.81	0.91	0.94	0.87	0.90	1.01
B3	$\frac{\text{Southwell}}{\text{Meck}}$	0.99	0.62	0.97	0.96	0.63	0.99	1.00	0.62	0.62	0.95
	$\frac{\text{Massey}}{\text{Meck}}$	0.99	0.62	0.97	0.96	0.63	0.99	1.00	0.62	0.62	0.95
	$\frac{\text{Modified}}{\text{Meck}}$	0.99	0.62	0.96	0.96	0.62	0.98	0.99	0.62	0.61	0.95

In order for further evaluation of validity as well as accuracy of the Meck Plot predictions for the various considered cases, these predictions are compared with the estimates of the three Southwell (Southwell 1932), Massey (Massey 1963), and Modified (Trahair 1969) Plot methods by using the lateral displacement of the top flange (δ_L) as the commonly-used deformation variable in these three methods. The results of this comparison are tabulated in Table 9. The application as well as performance of the Southwell, Massey, and Modified plotting techniques have been discussed and evaluated elsewhere (Zirakian 2010); however, herein it is intended to make a comprehensive evaluation of accuracy of the Meck Plot predictions in the various cases by considering the estimates of these three established plotting techniques.

As it is seen in the table, in spite of some scatter in the results due to the application of various deformation variables and extrapolation techniques as well as consideration of various loading, cross-section, and support conditions, regardless of the few aforementioned cases of B3, the agreement between the predictions of the Meck Plot method with those of the other Plots is by and large satisfactory. Therefore, this indicates that the application of the Meck Plot method with the combination of various deformation variables may result in reliable and sufficiently accurate predictions for elastic lateral-distortional buckling of I-beams.

All in all, the findings of the present and prior studies indicate that the application of the extrapolation techniques for experimental determination of the critical buckling load of structures does not actually need to be limited to the use of certain and just a few deformation variables, since it has been shown that the various deformation variables of structures may be directly coupled with each other and consequently yield similar and acceptable predictions.

6. Conclusions

The proportionality between various deformation variables including the web transverse and longitudinal strains, vertical deflection, and angles of twist of top and bottom flanges of I-beams undergoing elastic lateral-distortional buckling with initial geometrical imperfections is investigated comprehensively in ten different cases as well as three different beam configurations with various loading, cross-section, and support conditions, and it is found that in all cases deformation variables are directly coupled.

By extending the lateral-torsional buckling theoretical model to the case of lateral-distortional buckling, regardless of a few cases, the proportionality between the various deformation variables is verified theoretically as well.

Ultimately, the Meck Plot method is applied on the various combinations of the different deformation variables, and consequently good predictions are generally obtained in all considered cases except a few cases of the cantilever beam where the vertical deflection is used with the other deformation variables.

References

- ABAQUS (2005), *ABAQUS Analysis User's Manual*, Ver. 6.5, ABAQUS, Inc.
- Mandal, P. and Calladine, C.R. (2002), "Lateral-torsional buckling of beams and the Southwell Plot", *Int. J. Mech. Sci.*, **44**, 2557-2571.
- Massey, C. (1963), "Elastic and inelastic lateral instability of I-beams", *Engineer*, **216**, 672-674.
- Meck, H.R. (1977), "Experimental evaluation of lateral buckling loads", *J. Eng. Mech. Div.-ASCE*, **103**, 331-337.
- Southwell, R.V. (1932), "On the analysis of experimental observations in the problems of elastic stability", *Proc. Roy. Philos. Soc. Lond.*, **135(A)**, 601.
- Trahair, N.S. (1969), "Deformations of geometrically imperfect beams", *J. Struct. Div.-ASCE*, **95(7)**, 1475-1496.
- Zirakian, T. (2008), "Lateral-distortional buckling of I-beams and the extrapolation techniques", *J. Constr. Steel Res.*, **64(1)**, 1-11.
- Zirakian, T. (2010), "On the application of the extrapolation techniques in elastic buckling", *J. Constr. Steel Res.*, **66(3)**, 335-341.

Notations

b_{fb}	: bottom flange width
b_{ft}	: top flange width
E	: Young's modulus of elasticity
F_y	: yield stress
G	: shear modulus of elasticity
h_w	: distance between flange centroids
L	: length of beam
M	: applied major axis end moment
M_{cr}	: critical value of M
M_{LDB}	: lateral-distortional buckling moment
M_{LTB}	: lateral-torsional buckling moment
M_{Meck}	: extrapolated critical moment obtained from Meck Plot
M_u	: ultimate failure moment
M_y	: yield moment
P	: point load applied at the free end of the cantilever beam
P_{Meck}	: point load obtained from Meck Plot
P_u	: ultimate failure point load
R	: Pearson product moment correlation coefficient
q	: intensity of the uniformly distributed load acting on the fixed-ended beam
q_{Meck}	: intensity of the uniformly distributed load obtained from Meck Plot
q_u	: intensity of the ultimate failure uniformly distributed load
t_f	: flange thickness
t_w	: web thickness
α	: reciprocal slope of the straight-line portions of plots of $d.v.2/M$ versus $d.v.1$
β	: reciprocal slope of the straight-line portions of plots of $d.v.1/M$ versus $d.v.2$
δ_L	: lateral displacement of the beam
δ_{Lc}	: lateral displacement at the center of the beam, measured from the unloaded configuration
δ_{Lo}	: initial lateral displacement (imperfection)
δ_V	: vertical (in-plane) deflection of the beam
δ_{Vo}	: initial vertical displacement (imperfection)
ϵ_L	: web longitudinal strain, measured at mid-height
ϵ_T	: web transverse strain, measured at mid-height
ϕ	: rotation of the section in lateral-torsional buckling mode
ϕ_c	: rotation of the section at the center of the beam, measured from unloaded configuration in lateral-torsional buckling mode
ϕ_o	: initial twist (imperfection)
ν	: Poisson's ratio
θ_{BF}	: angle of twist of bottom flange
θ_{TF}	: angle of twist of top flange